Author Manuscript Published OnlineFirst on December 2, 2013; DOI: 10.1158/1541-7786.MCR-13-0258-T
Author manuscripts have been peer reviewed and accepted for publication but have not yet been edited.

Molecular Cancer Research

Autophagy-Dependent Metabolic Reprogramming Sensitizes TSC2-Deficient Cells to the Antimetabolite 6-Aminonicotinamide

Andrey A. Parkhitko, Carmen Priolo, Jonathan L. Coloff, et al.

Mol Cancer Res Published OnlineFirst December 2, 2013.

Updated version	Access the most recent version of this article at: doi:10.1158/1541-7786.MCR-13-0258-T
Supplementary Material	Access the most recent supplemental material at: http://mcr.aacrjournals.org/content/suppl/2013/12/02/1541-7786.MCR-13-0258-T.DC1.html
Author Manuscript	Author manuscripts have been peer reviewed and accepted for publication but have not yet been edited.

E-mail alerts	Sign up to receive free email-alerts related to this article or journal.
Reprints and Subscriptions	To order reprints of this article or to subscribe to the journal, contact the AACR Publications Department at pubs@aacr.org.
Permissions	To request permission to re-use all or part of this article, contact the AACR Publications Department at permissions@aacr.org.

Downloaded from mcr.aacrjournals.org on December 28, 2013. © 2013 American Association for Cancer Research.

Author Manuscript Published OnlineFirst on December 2, 2013; DOI: 10.1158/1541-7786.MCR-13-0258-T
Author manuscripts have been peer reviewed and accepted for publication but have not yet been edited.

Autophagy-Dependent Metabolic Reprogramming Sensitizes TSC2-Deficient Cells to the Antimetabolite 6-Aminonicotinamide

Andrey A. Parkhitko[1,5,7*], Carmen Priolo[1,5*], Jonathan L. Coloff[2], Jihye Yun[3,5], Julia J. Wu[6], Kenji Mizumura[1,5], Wenping Xu[1,5], Izabela A. Malinowska[4,5], Jane Yu[1,5], David J. Kwiatkowski[4,5], Jason W. Locasale[8], John M. Asara[3], Augustine M. K. Choi[1], Toren Finkel[6], Elizabeth P. Henske[1]

[1]Division of Pulmonary and Critical Care Medicine, Brigham and Women's Hospital, [2]Department of Cell Biology, Harvard Medical School, [3]Division of Signal Transduction, Beth Israel Deaconess Medical Center, and [4]Division of Translational Medicine, Brigham and Women's Hospital, [5]Harvard Medical School, Boston, MA, [6]National Heart Lung and Blood Institute, [7]Russian State Medical University, Moscow, Russia, [8]Division of Nutritional Sciences, Cornell University, New York, NY

*The first two Authors contributed equally

Contact:

Elizabeth P. Henske, MD

Email: ehenske@partners.org; phone: (617)3559049; fax: (617)3559016.

Carmen Priolo, MD PhD

Email: cpriolo@partners.org; phone: (617)3559012; fax: (617)3559016.

Running Title

Autophagy and Glucose Metabolism

The authors disclose no potential conflicts of interest

Downloaded from mcr.aacrjournals.org on December 28, 2013. © 2013 American Association for Cancer Research.

Author Manuscript Published OnlineFirst on December 2, 2013; DOI: 10.1158/1541-7786.MCR-13-0258-T
Author manuscripts have been peer reviewed and accepted for publication but have not yet been edited.

Abstract

The mammalian target of rapamycin complex 1 (mTORC1) is hyperactive in many human cancers and in tuberous sclerosis complex (TSC). Autophagy, a key mTORC1 targeted process, is a critical determinant of metabolic homeostasis. Metabolomic profiling was performed to elucidate the cellular consequences of autophagy dysregulation under conditions of hyperactive mTORC1. It was discovered that TSC2-null cells have distinctive autophagy-dependent pentose phosphate pathway (PPP) alterations. This was accompanied by enhanced glucose uptake and utilization, decreased mitochondrial oxygen consumption, and increased mitochondrial ROS production. Importantly, these findings revealed that the PPP is a key autophagy-dependent compensatory metabolic mechanism. Furthermore, PPP inhibition with 6-aminonicotinamide (6-AN) in combination with autophagy inhibition suppressed proliferation and prompted the activation of NF-kB and CASP1 in TSC2-deficient, but not TSC2-proficient cells. These data demonstrate that TSC2-deficient cells can be therapeutically targeted, without mTORC1 inhibitors, by focusing on their metabolic vulnerabilities. Implications: This study provides proof-of-concept that therapeutic targeting of diseases with hyperactive mTORC1 can be achieved without the application of mTORC1 inhibitors.

Downloaded from mcr.aacrjournals.org on December 28, 2013. © 2013 American Association for Cancer Research.

Author Manuscript Published OnlineFirst on December 2, 2013; DOI: 10.1158/1541-7786.MCR-13-0258-T
Author manuscripts have been peer reviewed and accepted for publication but have not yet been edited.

Introduction

Autophagy is a catabolic process leading to the degradation of cytoplasmic content in lysosomal compartments, thereby providing an endogenous source of nutrients for energy production under stress conditions and allowing dysfunctional organelles, including mitochondria, to be "recycled" [1]. Tumor cells often upregulate autophagy to promote survival and drug resistance [2]. The role of autophagy in cancer therapy is an area of active clinical investigation.

Tuberous sclerosis complex (TSC) is an autosomal dominant syndrome caused by germline mutations of the *TSC1* and *TSC2* tumor suppressor genes [3]. TSC patients develop histologically benign but life-threatening proliferative lesions in multiple organs, including the brain, heart, lung and kidney. The *TSC1* and *TSC2* gene products form a complex that suppresses mammalian target of rapamycin complex 1 (mTORC1). mTORC1 is a major regulator of protein translation, autophagy and metabolism. Hyperactive mTORC1 occurs in the tumors that develop in TSC patients and in many human cancers, leading to differential metabolic requirements in the setting of low autophagy levels [4, 5].

Autophagy inhibition has been shown to suppress the growth of tumor cells [6]. We previously found that constitutive activation of mTORC1 in TSC2-null cells leads to decreased levels of basal and stress-induced autophagy, and increases their vulnerability to further autophagy inhibition [7], yet the metabolic consequences of autophagy inhibition in the context of hyperactive mTORC1 are not fully understood. Moreover, the metabolic pathways utilized by tumor cells to maintain growth and survival when autophagy is inhibited are poorly characterized. We report here that the metabolic reprogramming induced by autophagy inhibition leads to pentose phosphate pathway "addiction" selectively in *Tsc2*-deficient cells. We also

Downloaded from mcr.aacrjournals.org on December 28, 2013. © 2013 American Association for Cancer Research.

Author Manuscript Published OnlineFirst on December 2, 2013; DOI: 10.1158/1541-7786.MCR-13-0258-T
Author manuscripts have been peer reviewed and accepted for publication but have not yet been edited.

provide proof-of-concept that the metabolic consequences of mTORC1 hyperactivation can be therapeutically targeted without inhibiting mTORC1 itself, thereby revealing novel therapeutic strategies for TSC.

Experimental Procedures

Cell lines

Tsc2$^{+/+}$*p53*$^{-/-}$ and *Tsc2*$^{-/-}$*p53*$^{-/-}$ MEFs were the gift of David Kwiatkowski and were confirmed to exhibit Tsc2 deficiency and constitutive activation of mTORC1 by immunoblotting of tuberin. Tsc2 deficiency and constitutive activation of mTORC1 were confirmed by immunoblotting of tuberin and phospho-S6, respectively. The novel *Tsc2*-null cystadenoma cell line, 105K, was derived from a *Tsc2*$^{+/-}$ C57Bl/6 mouse renal tumor and isolated in the laboratory of Dr. Elizabeth Henske. These cells were confirmed to have loss of the second allele of *Tsc2* by PCR**,** loss of tuberin expression and increased phospho-S6 levels by immunoblotting. All cells were cultured in DMEM supplemented with 10% FBS, 100 μg/mL penicillin and 100 μg/mL streptomycin.

Drugs and shRNA

Chloroquine diphosphate salt, bafilomycin A and 6-aminonicotinamide were obtained from Sigma-Aldrich. Spautin-1 was obtained from Cellagen Technology. Short hairpin RNAs (shRNAs) against Atg-5 (TRCN0000099434 and TRCN0000099431), LAMP2a (TRCN0000086974), Beclin1 (TRCN0000087290) or control (shGFP) were obtained from the RNAi Consortium (TRC).

Mice

Downloaded from mcr.aacrjournals.org on December 28, 2013. © 2013 American Association for Cancer Research.

Author Manuscript Published OnlineFirst on December 2, 2013; DOI: 10.1158/1541-7786.MCR-13-0258-T
Author manuscripts have been peer reviewed and accepted for publication but have not yet been edited.

Tsc2$^{+/-}$ mice were studied in the A/J genetic background. The severity of renal lesions in the *Tsc2*$^{+/-}$ mice was scored using a quantitative index as previously described[8], incorporating standardized gross inspection and microscopic histological parameters. The animal studies were approved by the Children's Hospital Boston Animal Care and Use Committee.

Metabolite profiling

Cells were harvested in quadruplicate, and intracellular metabolites extracted using 4 mL of cold (-80°C) 80% (v/v) aqueous methanol. Cells and the metabolite-containing supernatants were collected into conical tubes. Insoluble material in lysates was centrifuged at 2,000*g* for 15 min, and the resulting supernatant was evaporated using a refrigerated speed vac. Samples were re-suspended using 20 µL HPLC grade water for mass spectrometry. 10 µL were injected and analyzed using a 5500 QTRAP triple quadrupole mass spectrometer (AB/SCIEX) coupled to a Prominence UFLC HPLC system (Shimadzu) via selected reaction monitoring (SRM) of a total of 254 endogenous water soluble metabolites for steady-state analyses of samples. Some metabolites were targeted in both positive and negative ion mode for a total of 287 SRM transitions using pos/neg polarity switching. ESI voltage was +4900V in positive ion mode and –4500V in negative ion mode. The dwell time was 3 ms per SRM transition and the total cycle time was 1.55 seconds. Approximately 10-14 data points were acquired per detected metabolite. Samples were delivered to the MS via normal phase chromatography using a 4.6 mm i.d x 10 cm Amide Xbridge HILIC column (Waters Corp.) at 350 µL/min. Gradients were run starting from 85% buffer B (HPLC grade acetonitrile) to 42% B from 0-5 minutes; 42% B to 0% B from 5-16 minutes; 0% B was held from 16-24 minutes; 0% B to 85% B from 24-25 minutes; 85% B was held for 7 minutes to re-equilibrate the column. Buffer A was comprised of 20 mM ammonium

Downloaded from mcr.aacrjournals.org on December 28, 2013. © 2013 American Association for Cancer Research.

Author Manuscript Published OnlineFirst on December 2, 2013; DOI: 10.1158/1541-7786.MCR-13-0258-T
Author manuscripts have been peer reviewed and accepted for publication but have not yet been edited.

hydroxide/20 mM ammonium acetate (pH=9.0) in 95:5 water:acetonitrile. Peak areas from the total ion current for each metabolite SRM transition were integrated using MultiQuant v2.0 software (AB/SCIEX).

The resulting raw data from the MultiQuant software were normalized by total proteins and then uploaded in metaboanalyst (http://www.metaboanalyst.ca/MetaboAnalyst/) for subsequent data processing and analyses. Raw and normalized/processed data are reported in Table S1. Metabolites that were not detected in at least one sample were excluded from the analysis. Data were normalized to the median (per sample) and processed through log transformation. Heat map and hierarchical clustering was generated using Pearson correlations and Ward's method. Metabolite Set Enrichment Analysis (MSEA) was performed using Metaboanalyst which exploits the KEGG (http://www.genome.jp/kegg/pathway.html) pathway database. Fifty-eight metabolites significantly increased in Tsc2-/- MEF with chloroquine treatment compared to vehicle ($p<0.05$, calculated by student t-test with univariate analysis and equal group variation) were used for MSEA analysis. For reference metabolites, total 235 metabolites were used. Metabolite sets containing at least 5 compounds were employed in the analysis. MSEA calculates hypergeometrics test score based on cumulative binominal distribution. Only 3 metabolites were found increased in Tsc2+/+ MEFs upon chloroquine treatment.

Nutrient consumption

Metabolite levels in the medium were measured using the Yellow Springs Instruments (YSI) 7100 as previously described [9].

Glucose and fatty acid oxidation

Downloaded from mcr.aacrjournals.org on December 28, 2013. © 2013 American Association for Cancer Research.

Author Manuscript Published OnlineFirst on December 2, 2013; DOI: 10.1158/1541-7786.MCR-13-0258-T
Author manuscripts have been peer reviewed and accepted for publication but have not yet been edited.

Cells were seeded in 12-well plates, treated for 24 hours, and incubated for 3 hours at 37°C with either 1 μCi/ml of [14C(U)]-labeled D-glucose or [14C(U)]-labeled palmitate (American Radiolabelled Chemicals Inc., St. Louis, MO). 3M perchloric acid was then added to the culture media and the dishes sealed with phenylethylamine (Sigma-Aldrich)-saturated Whatman filter paper to capture ^{14}C-CO2, as previously described [10]. Following 3-hour incubation at room temperature on a gentle shaker, the filter paper was removed, placed into Ultima Gold F Scintillation Fluid (PerkinElmer Inc.), and radioactivity counts (CPM) were read in a 1600 liquid scintillation analyzer (Packard).

Oxygen consumption

Oxygen consumption was measured under basal conditions or in the presence of the FCCP using the Seahorse Bioscience XF24 analyzer as previously described [7]. Levels of oxygen consumption were normalized to cell number.

ROS production

Mitochondrial ROS were measured by using MitoSOX (Invitrogen) staining (5mM for 15 minutes at 37º). Cells were washed with PBS, trypsinized and resuspended in PBS containing 1% FBS. Data were acquired with a BD FACS Canto II flow cytometer (BD Biosciences) and analyzed with FlowJo analytical software (Treestar) [11].

Crystal violet staining

Cells were plated into 96-well plates (1000 cells/well). After treatment, cells were fixed with 10% formalin for 5 minutes, stained with 0.05% crystal violet in distilled water for 30 minutes,

Downloaded from mcr.aacrjournals.org on December 28, 2013. © 2013 American Association for Cancer Research.

Author Manuscript Published OnlineFirst on December 2, 2013; DOI: 10.1158/1541-7786.MCR-13-0258-T
Author manuscripts have been peer reviewed and accepted for publication but have not yet been edited.

washed 2 times with tap water, and drained. Crystal violet was solubilized with 100 ul of methanol and the plate was read with a BioTek plate reader (OD 540).

Antibodies and Immunoblot Analysis

Phospho-S6 (Ser235/236), phospho-S6K (Thr 389), total S6, total S6K, phospho-4E-BP (Thr 37/46), total p65, β-actin and phospho-p65 antibodies were obtained from Cell Signaling Technology, tuberin antibody from Abcam, Beclin-1 and caspase-1 antibody from Santa Cruz, LC3 antibody from Novus Biologicals, Atg5 antibody from Sigma, LAMP2A antibody from Invitrogen. For immunoblot analyses, cells were washed with PBS and harvested in a lysis buffer containing Nonidet P-40. Whole-cell lysates were resolved by electrophoresis, and proteins were transferred onto PVDF membrane (Immobilon P; Millipore), blocked in Tris-buffered saline Tween-20 buffer (Cell Signaling Technology), and probed with the indicated antibodies in this buffer.

IL-6 measurement

IL-6 levels were measured in the conditioned media using a Luminex LX100 instrument.

Statistics

One-sample and Two-sample t-tests, and the Mann-Whitney test were used for *in vitro* and *in vivo* studies (GraphPad Prism version 5.04 for Windows, GraphPad Software, San Diego California USA, www.graphpad.com). Significance was defined as $p<0.05$. Data are shown as means ± SD.

Downloaded from mcr.aacrjournals.org on December 28, 2013. © 2013 American Association for Cancer Research.

Author Manuscript Published OnlineFirst on December 2, 2013; DOI: 10.1158/1541-7786.MCR-13-0258-T
Author manuscripts have been peer reviewed and accepted for publication but have not yet been edited.

Results

Autophagy inhibition suppresses proliferation and tumorigenesis of *Tsc2*-null cells and leads to metabolic reprogramming.

To investigate the impact of autophagy suppression on the proliferation and metabolism of cells with hyperactive mTORC1 signaling, we used chloroquine (CQ), which raises lysosomal pH and inhibits the fusion between autophagosomes and lysosomes, to treat *Tsc2*-deficient mouse embryonic fibroblasts (MEFs) in monolayer culture. Chloroquine partially suppressed cell proliferation (38% after 96 hr of treatment, $p<0.05$) (**Figures 1A** and **S1A**) in a TSC2-dependent manner (**Figure 1A**). Next, we treated $Tsc2^{+/-}$ mice, which develop spontaneous renal cystadenomas, with chloroquine (50 mg/kg/day, i.p., 5 days/week) for 4 months. Chloroquine decreased the number of macroscopic and microscopic renal lesions by ~50% (**Figure 1B).** Chloroquine treatment did not affect body weight (**Figure S1B**).

To identify compensatory metabolic mechanisms activated upon suppression of autophagy, metabolite profiling of *Tsc2*-null MEFs treated with chloroquine (5μM) was performed. Chloroquine induced extensive alterations including changes in the glucose, amino acid and nucleotide utilization/biosynthesis pathways (**Figure 1C** and **Table S1**). Importantly, mTORC1 activity was not affected by chloroquine as assessed by the phosphorylation of ribosomal protein S6 (**Figure 1C**). Metabolite Set Enrichment Analysis (MSEA) applied to metabolites whose levels increased in chloroquine-treated *Tsc2*-null cells identified the pentose phosphate pathway as the most enriched metabolic pathway (**Figure 1C, D**). In contrast, metabolites of the PPP pathway were either unchanged or decreased upon treatment with chloroquine in $Tsc2^{+/+}$ cells (**Figure S2** and **Table S1**).

Downloaded from mcr.aacrjournals.org on December 28, 2013. © 2013 American Association for Cancer Research.

Author Manuscript Published OnlineFirst on December 2, 2013; DOI: 10.1158/1541-7786.MCR-13-0258-T
Author manuscripts have been peer reviewed and accepted for publication but have not yet been edited.

Autophagy inhibition enhances glucose uptake and glucose oxidative metabolism via non-mitochondrial pathways.

We next measured uptake of glucose and secretion of lactate in *Tsc2*$^{-/-}$ and *Tsc2*$^{+/+}$ MEFs treated for 24 hr with chloroquine (CQ). Interestingly, glucose uptake was significantly increased by CQ in *Tsc2*-null cells ($p<0.05$, **Figure 2A**) but not *Tsc2*$^{+/+}$ cells. The amount of lactate in the media was unchanged, indicating that the CQ-induced glucose uptake in *Tsc2*$^{-/-}$ cells is not associated with increased aerobic glycolysis. *Tsc2*$^{-/-}$ MEFs in which the autophagy gene *Atg5* or *Beclin 1* (*Atg6*) was inhibited by shRNA also exhibited significantly higher glucose consumption relative to control shRNA, with no increase in lactate secretion (**Figure 2A** and **S3**), consistent with the CQ results.

To define the metabolic routes to which glucose is directed when autophagy is inhibited, we assayed oxidative metabolism. First, we measured the oxygen consumption rate of cells treated with chloroquine. Following 24 hr treatment with CQ, *Tsc2*$^{-/-}$ MEFs displayed a significant suppression of both basal and maximal (FCCP induced) oxygen consumption rate (**Figure 2B**), consistent with our previous results in *Tsc2*-null rat leiomyoma ELT3 cells [7]. A concomitant increase in mitochondrial ROS was observed in *Tsc2*$^{-/-}$ MEFs treated with chloroquine for 24 hr (**Figure S4**) suggesting progressive accumulation of damaged mitochondria.

Next, we dissected changes in oxidative utilization of individual nutrients by measuring ^{14}C-CO_2 release from cells labeled for 3 hr with D[U-^{14}C]glucose or [U-^{14}C]palmitate. Consistent with the metabolomic results, chloroquine induced an increase in glucose oxidation selectively in *Tsc2*-null cells ($p<0.05$, **Figure 3A, D**). In addition, fatty acid oxidation decreased in chloroquine–treated *Tsc2*-null cells ($p<0.05$, **Figure 3B, D**), consistent with the reduction in

Downloaded from mcr.aacrjournals.org on December 28, 2013. © 2013 American Association for Cancer Research.

Author Manuscript Published OnlineFirst on December 2, 2013; DOI: 10.1158/1541-7786.MCR-13-0258-T
Author manuscripts have been peer reviewed and accepted for publication but have not yet been edited.

oxygen consumption rate. Treatment with Rapamycin markedly reduced glucose oxidation even in the presence of CQ ($p<0.05$, **Figure 3C**), suggesting mTORC1-dependence.

Together, these results suggest that autophagy inhibition in *Tsc2*-null cells leads to increased glucose utilization via the pentose phosphate pathway, coupled with decreased oxygen consumption, in an mTORC1-dependent manner.

Autophagy inhibition sensitizes *Tsc2*-null cells to 6-aminonicotinamide.

Based on the above results, we hypothesized that *Tsc2*-null cells become dependent on the pentose phosphate pathway under autophagy inhibition. To test this hypothesis, we used the antimetabolite 6-aminonicotinamide (6-AN), a competitive inhibitor of glucose-6-phosphate dehydrogenase (G6PD) and 6-phosphogluconate dehydrogenase (6PGD), the two key enzymes of the oxidative branch of the pentose phosphate pathway. G6PD catalyzes the conversion of glucose-6-phosphate into 6-phosphogluconolactone, which is the rate-limiting step of the pentose phosphate shunt, and 6PGD the subsequent oxidation of 6-phosphogluconolactone. Cells were treated with chloroquine, 6-AN or both drugs for 96 hr. Strikingly, the chloroquine/6-AN combination selectively inhibited the proliferation of *Tsc2*$^{-/-}$ cells (**Figure 4A, B**). No consistent effect on mTORC1 signaling was noted (**Figure S5A**). To validate these results, we used a mechanistically distinct inhibitor of autophagy, spautin-1, which promotes the proteasomal degradation of Beclin 1 [12]. Consistent with the chloroquine results, treatment with the combination of spautin-1 and 6-AN selectively inhibited the proliferation of *Tsc2*$^{-/-}$ cells (**Figure 4C**). In addition, 6-AN treatment of cells infected with either *Atg5* or *LAMP2a* (a chaperone-mediated autophagy gene) shRNA decreased proliferation of *Tsc2*$^{-/-}$ cells compared to control shRNA (**Figure 5**). The addition of rapamycin did not further affect proliferation in the presence

Downloaded from mcr.aacrjournals.org on December 28, 2013. © 2013 American Association for Cancer Research.

Author Manuscript Published OnlineFirst on December 2, 2013; DOI: 10.1158/1541-7786.MCR-13-0258-T
Author manuscripts have been peer reviewed and accepted for publication but have not yet been edited.

of CQ and 6-AN (**Figure S5B**). The pentose phosphate pathway generates ribose-5-phosphate and NADPH. Interestingly, supplementation with 0.1 mM NADPH [13] was sufficient to sustain the proliferation of *Tsc2*$^{-/-}$ cells during treatment with the combination of chloroquine and 6-AN (**Figure 4D**), suggesting that production of NADPH via pentose phosphate pathway is essential to the proliferation of *Tsc2*$^{-/-}$ cells.

The combination of chloroquine and 6-AN suppressed the proliferation of a novel *Tsc2*-null cystadenoma cell line, named 105K (**Figure S6**), similarly to the *Tsc2*$^{-/-}$ MEFs. These cells were derived from a *Tsc2*$^{+/-}$ C57Bl/6 mouse renal tumor, and confirmed to have loss of the second allele of *Tsc2* gene (Figure S6), loss of tuberin expression, increased phospho-S6 levels, and decreased levels of autophagy (measured by p62 accumulation) (Figure S6).

Combined autophagy and pentose phosphate pathway inhibition leads to activation of NF-kB and inflammasome pathways.

We found that chloroquine treatment led to an increase in ROS levels in *Tsc2-/-* MEFs (Figure S4), which, together with cytosolic release of mitochondrial DNA due to impaired mitophagy [14], may activate NF-kB/Rel activity [15]. Consistent with this reasoning, phosphorylation of p65/RelA was induced at 96 hours by the combination of chloroquine and 6-AN (**Figure 6A**), associated with increased secretion of IL-6, a known transcriptional target of NF-kB (**Figure S7)**. IL-6 was not detectable in *Tsc2*$^{+/+}$ control cells at baseline or after treatment with CQ/6-AN (Figure S7). Furthermore, we observed accumulation of cleaved-caspase-1, a marker of inflammasome activation, under the combined CQ/6-AN treatment at 96 hours (**Figure 6B**). Supplementation with 0.1 mM NADPH was sufficient to prevent accumulation of

Downloaded from mcr.aacrjournals.org on December 28, 2013. © 2013 American Association for Cancer Research.

Author Manuscript Published OnlineFirst on December 2, 2013; DOI: 10.1158/1541-7786.MCR-13-0258-T
Author manuscripts have been peer reviewed and accepted for publication but have not yet been edited.

cleaved-caspase-1 under CQ/6-AN treatment for 96 hours (**Figure 6C**), consistent with the rescue of cell proliferation by NADPH (Figure 4D).

To test the hypothesis that activation of NF-kB is necessary for the inhibition of cell proliferation by chloroquine and 6-AN, we treated the cells with parthenolide, which inhibits both p65/RelA and caspase-1 via alkylation [16]. Parthenolide restored proliferation in cells treated with CQ and 6-AN (**Figure S8**). These data suggest that the combination of chloroquine and 6-AN inhibits the proliferation of *Tsc2*-null cells via ROS-dependent activation of NF-kB and caspase-1.

Discussion

Chloroquine and its analog hydroxychloroquine, which block lysosome-autophagosome fusion and lysosomal function thus suppressing macroautophagy and chaperone-mediated autophagy, can inhibit cancer cell survival under stress conditions [1]. We report here that prolonged (4 month) treatment with chloroquine suppressed the number and size of renal tumors in $Tsc2^{+/-}$ mice, consistent with the decreased spontaneous renal tumors we previously observed in *Tsc2*/*Beclin1* double heterozygous mice [7]. We hypothesized that metabolic compensatory mechanisms are activated when autophagy is suppressed by chloroquine in *Tsc2*-deficient cells, thereby preventing a more complete therapeutic response. Metabolite profiling revealed striking changes in the metabolome of *Tsc2*-null cells treated with chloroquine, including increased levels of five pentose phosphate pathway intermediate metabolites. Isotope labeling experiments revealed an increase in glucose oxidation under chloroquine treatment, which may reflect activation of the oxidative branch of the pentose phosphate pathway. The pentose phosphate shunt, which is often upregulated in cancer, has both biosynthetic and oxidative functions,

Downloaded from mcr.aacrjournals.org on December 28, 2013. © 2013 American Association for Cancer Research.

Author Manuscript Published OnlineFirst on December 2, 2013; DOI: 10.1158/1541-7786.MCR-13-0258-T
Author manuscripts have been peer reviewed and accepted for publication but have not yet been edited.

representing the main source of NADPH via its oxidative branch and supplying ribose-5 phosphate for nucleotide synthesis.

In parallel with the pentose phosphate pathway upregulation, we found that chloroquine induced ROS production at a higher rate in *Tsc2*-null cells than in cells with intact TSC2. This could be due to impaired mitophagy and subsequent accumulation of dysfunctional mitochondria, which would increase the cell requirement for reducing power to buffer elevated ROS production. TSC2-deficient cells may be particularly vulnerable to loss of reducing power, since they are known to produce elevated amounts of ROS at baseline [17] and to be highly sensitive to increased ROS [18].

Therefore, these data suggest that the pentose phosphate pathway becomes a crucial metabolic survival mechanism in TSC2-null cells when they encounter the increase in oxidative stress due to further autophagy suppression. To test this hypothesis, we used the anti-metabolite 6-AN, which inhibits the pentose phosphate pathway-dependent NADPH supply [19], in combination with chloroquine. The CQ/6-AN combination dramatically suppressed the proliferation of *Tsc2*-null cells, which was rescued by supplementation of NADPH. Similar results were seen with spautin-1 [12], a recently reported inhibitor of Beclin-1, and with downregulation of Atg5 and Lamp2a genes, supporting the hypothesis that the effect of chloroquine in these experiments is autophagy-mediated. Spautin-1 has been found to induce cell death under glucose deprivation conditions in breast cancer cells [12], further underscoring the links between the metabolic status of tumor cells and their response to autophagy inhibition.

Notably, the combination of chloroquine and 6-AN triggered activation of the NF-kB and inflammasome pathways in a TSC2-dependent manner, and parthenolide [16], which inhibits both NF-kB and caspase-1, rescued proliferation under these conditions. Inflammasomes are

Downloaded from mcr.aacrjournals.org on December 28, 2013. © 2013 American Association for Cancer Research.

Author Manuscript Published OnlineFirst on December 2, 2013; DOI: 10.1158/1541-7786.MCR-13-0258-T
Author manuscripts have been peer reviewed and accepted for publication but have not yet been edited.

multiprotein complexes that mediate the cleavage and activation of caspase-1, thereby stimulating an inflammatory response and/or programmed cell death [20]. Multiple factors can activate the inflammasome, including autophagy inhibition, mitochondrial DNA release, increased ROS and activation of NF-kB [15, 21], thus affecting cell survival/proliferation. Recent work has linked the NF-kB pathway to the immune response and cellular senescence and has suggested that NF-kB may serve a tumor suppressor function in some circumstances. Together, our results lead us to the conclusion that the inhibition of autophagy and the pentose phosphate pathway leads to depletion of NADPH, increased ROS production and activation of NF-kB/Rel. We propose that this ultimately suppresses cell proliferation via activation of the inflammasome (**Figure 6D**).

Our results point toward novel therapeutic strategies for neoplasms with mTORC1 activation by targeting their intrinsic dependence on autophagy and the metabolic compensatory mechanisms triggered by autophagy inhibition. Thus, in TSC and related diseases, including lymphangioleiomyomatosis (LAM), our data provide a first proof-of-concept that therapeutic targeting of cells with hyperactive mTORC1 can be accomplished by targeting their metabolic vulnerabilities without the utilization of mTORC1 inhibitors. We note that the autophagy inhibitors chloroquine and hydroxychloroquine (Plaquenil) are currently being tested in clinical trials for multiple types of cancer and for LAM, and a novel derivative of chloroquine with higher efficacy *in vitro* and *in vivo* [22] has been recently synthesized. Furthermore, more than 100 cancer trials using "Rapalogs" and other mTORC1 inhibitors are currently enrolling patients, yet durable clinical responses are uncommon. Therefore, novel approaches targeting the metabolism of tumors with mTORC1 activation may have broad clinical impact.

Downloaded from mcr.aacrjournals.org on December 28, 2013. © 2013 American Association for Cancer Research.

Author Manuscript Published OnlineFirst on December 2, 2013; DOI: 10.1158/1541-7786.MCR-13-0258-T
Author manuscripts have been peer reviewed and accepted for publication but have not yet been edited.

References

1. Singh R, Cuervo AM: Autophagy in the cellular energetic balance, Cell Metab 2011, 13:495-504

2. White E: Deconvoluting the context-dependent role for autophagy in cancer, Nat Rev Cancer 2012, 12:401-410

3. Crino PB, Nathanson KL, Henske EP: The tuberous sclerosis complex, N Engl J Med 2006, 355:1345-1356

4. Choo AY, Kim SG, Vander Heiden MG, Mahoney SJ, Vu H, Yoon SO, Cantley LC, Blenis J: Glucose addiction of TSC null cells is caused by failed mTORC1-dependent balancing of metabolic demand with supply, Mol Cell 2010, 38:487-499

5. Duvel K, Yecies JL, Menon S, Raman P, Lipovsky AI, Souza AL, Triantafellow E, Ma Q, Gorski R, Cleaver S, Vander Heiden MG, MacKeigan JP, Finan PM, Clish CB, Murphy LO, Manning BD: Activation of a metabolic gene regulatory network downstream of mTOR complex 1, Mol Cell 2010, 39:171-183

6. Guo JY, Chen HY, Mathew R, Fan J, Strohecker AM, Karsli-Uzunbas G, Kamphorst JJ, Chen G, Lemons JM, Karantza V, Coller HA, Dipaola RS, Gelinas C, Rabinowitz JD, White E: Activated Ras requires autophagy to maintain oxidative metabolism and tumorigenesis, Genes Dev 2011, 25:460-470

7. Parkhitko A, Myachina F, Morrison TA, Hindi KM, Auricchio N, Karbowniczek M, Wu JJ, Finkel T, Kwiatkowski DJ, Yu JJ, Henske EP: Tumorigenesis in tuberous sclerosis complex is autophagy and p62/sequestosome 1 (SQSTM1)-dependent, Proc Natl Acad Sci U S A 2011, 108:12455-12460

Downloaded from mcr.aacrjournals.org on December 28, 2013. © 2013 American Association for Cancer Research.

Author Manuscript Published OnlineFirst on December 2, 2013; DOI: 10.1158/1541-7786.MCR-13-0258-T
Author manuscripts have been peer reviewed and accepted for publication but have not yet been edited.

8. Pollizzi K, Malinowska-Kolodziej I, Stumm M, Lane H, Kwiatkowski D: Equivalent benefit of mTORC1 blockade and combined PI3K-mTOR blockade in a mouse model of tuberous sclerosis, Mol Cancer 2009, 8:38

9. Ying H, Kimmelman AC, Lyssiotis CA, Hua S, Chu GC, Fletcher-Sananikone E, Locasale JW, Son J, Zhang H, Coloff JL, Yan H, Wang W, Chen S, Viale A, Zheng H, Paik JH, Lim C, Guimaraes AR, Martin ES, Chang J, Hezel AF, Perry SR, Hu J, Gan B, Xiao Y, Asara JM, Weissleder R, Wang YA, Chin L, Cantley LC, DePinho RA: Oncogenic Kras maintains pancreatic tumors through regulation of anabolic glucose metabolism, Cell 2012, 149:656-670

10. Gerhart-Hines Z, Rodgers JT, Bare O, Lerin C, Kim SH, Mostoslavsky R, Alt FW, Wu Z, Puigserver P: Metabolic control of muscle mitochondrial function and fatty acid oxidation through SIRT1/PGC-1alpha, EMBO J 2007, 26:1913-1923

11. Nakahira K, Haspel JA, Rathinam VA, Lee SJ, Dolinay T, Lam HC, Englert JA, Rabinovitch M, Cernadas M, Kim HP, Fitzgerald KA, Ryter SW, Choi AM: Autophagy proteins regulate innate immune responses by inhibiting the release of mitochondrial DNA mediated by the NALP3 inflammasome, Nat Immunol 2011, 12:222-230

12. Liu J, Xia H, Kim M, Xu L, Li Y, Zhang L, Cai Y, Norberg HV, Zhang T, Furuya T, Jin M, Zhu Z, Wang H, Yu J, Hao Y, Choi A, Ke H, Ma D, Yuan J: Beclin1 controls the levels of p53 by regulating the deubiquitination activity of USP10 and USP13, Cell 2011, 147:223-234

13. Lu H, Waxman DJ: Antitumor activity of methoxymorpholinyl doxorubicin: potentiation by cytochrome P450 3A metabolism, Mol Pharmacol 2005, 67:212-219

14. Oka T, Hikoso S, Yamaguchi O, Taneike M, Takeda T, Tamai T, Oyabu J, Murakawa T, Nakayama H, Nishida K, Akira S, Yamamoto A, Komuro I, Otsu K: Mitochondrial DNA that escapes from autophagy causes inflammation and heart failure, Nature 2012, 485:251-255

Downloaded from mcr.aacrjournals.org on December 28, 2013. © 2013 American Association for Cancer Research.

Author Manuscript Published OnlineFirst on December 2, 2013; DOI: 10.1158/1541-7786.MCR-13-0258-T
Author manuscripts have been peer reviewed and accepted for publication but have not yet been edited.

15. Morgan MJ, Liu ZG: Crosstalk of reactive oxygen species and NF-kappaB signaling, Cell Res 2011, 21:103-115

16. Orofino Kreuger MR, Grootjans S, Biavatti MW, Vandenabeele P, D'Herde K: Sesquiterpene lactones as drugs with multiple targets in cancer treatment: focus on parthenolide, Anticancer Drugs 2012,

17. Finlay GA, Thannickal VJ, Fanburg BL, Kwiatkowski DJ: Platelet-derived growth factor-induced p42/44 mitogen-activated protein kinase activation and cellular growth is mediated by reactive oxygen species in the absence of TSC2/tuberin, Cancer Res 2005, 65:10881-10890

18. Li B, Gordon GM, Du CH, Xu J, Du W: Specific killing of Rb mutant cancer cells by inactivating TSC2, Cancer Cell 2010, 17:469-480

19. Hothersall JS, Gordge M, Noronha-Dutra AA: Inhibition of NADPH supply by 6-aminonicotinamide: effect on glutathione, nitric oxide and superoxide in J774 cells, FEBS Lett 1998, 434:97-100

20. Strowig T, Henao-Mejia J, Elinav E, Flavell R: Inflammasomes in health and disease, Nature 2012, 481:278-286

21. Saitoh T, Fujita N, Jang MH, Uematsu S, Yang BG, Satoh T, Omori H, Noda T, Yamamoto N, Komatsu M, Tanaka K, Kawai T, Tsujimura T, Takeuchi O, Yoshimori T, Akira S: Loss of the autophagy protein Atg16L1 enhances endotoxin-induced IL-1beta production, Nature 2008, 456:264-268

22. McAfee Q, Zhang Z, Samanta A, Levi SM, Ma XH, Piao S, Lynch JP, Uehara T, Sepulveda AR, Davis LE, Winkler JD, Amaravadi RK: Autophagy inhibitor Lys05 has single-

Downloaded from mcr.aacrjournals.org on December 28, 2013. © 2013 American Association for Cancer Research.

Author Manuscript Published OnlineFirst on December 2, 2013; DOI: 10.1158/1541-7786.MCR-13-0258-T
Author manuscripts have been peer reviewed and accepted for publication but have not yet been edited.

agent antitumor activity and reproduces the phenotype of a genetic autophagy deficiency, Proc Natl Acad Sci U S A 2012, 109:8253-8258

Acknowledgements

This work was supported by the LAM Foundation, the Adler Foundation, the Tuberous Sclerosis Alliance, the National Institute of Diabetes and Digestive and Kidney Diseases (to E.P.H.), the National Heart, Lung, and Blood Institute (to J.J.Y.), and the National Cancer Institute (to D.J.K.). We thank Min Yuan and Susanne Breitkopf for help with mass spectrometry experiments and grants NIH 5P01CA120964-04 and NIH DF/HCC Cancer Center Support Grant P30CA006516-46 (to J.M.A.). This research was conducted in partial fulfillment of A.P.'s doctoral degree requirements at the Department of Molecular Biology, Russian State Medical University, under the supervision of Dr. Olga Favorova.

Downloaded from mcr.aacrjournals.org on December 28, 2013. © 2013 American Association for Cancer Research.

Author Manuscript Published OnlineFirst on December 2, 2013; DOI: 10.1158/1541-7786.MCR-13-0258-T
Author manuscripts have been peer reviewed and accepted for publication but have not yet been edited.

Figure legends

Figure 1. Chloroquine inhibits the proliferation and tumorigenicity of Tsc2-deficient cells and reprograms their metabolism

(A) Proliferation of *Tsc2*$^{-/-}$ and *Tsc2*$^{+/+}$ MEFs treated with chloroquine (CQ, 5 μM) for 4 days (crystal violet staining). Time points represent average of 3 independent experiments ± SD. Comparison of *Tsc2*$^{-/-}$ treated with CQ vs. control: *p<0.05.

B) Macroscopic (upper panel) and microscopic (lower panel) score of spontaneous renal tumors in *Tsc2*$^{+/-}$ mice (n=15 for macroscopic and n=8 for microscopic score) following 4 month of i.p. treatment with chloroquine (CQ, 50 mg/kg/day, 5 days/week) or placebo (n=14 for macroscopic and n=14 for microscopic score). Photographs show representative kidneys of a control mouse and a CQ-treated mouse. Arrows indicate macroscopic lesions. **p<0.01

(C) Heat map showing the top 40 metabolites significantly changed in *Tsc2*$^{-/-}$ MEFs treated with Chloroquine (CQ, 5 μM) for 24 hours (n= 4 samples) versus control (n= 4 samples; left panel). Immunoblot analysis of phospho-S6 Ser 235/236 in *Tsc2*$^{-/-}$ MEFs treated with chloroquine (CQ, 5 μM) for 24 hours. Metabolic Set Enrichment Analysis (MSEA) of the *Tsc2*$^{-/-}$ MEFs treated with CQ vs. control (right panel).

(D) Box plots of individual pentose phosphate pathway metabolites that were significantly changed in *Tsc2*$^{-/-}$ MEFs treated with chloroquine (CQ, 5 μM) for 24 hours.

Figure 2. Autophagy inhibition enhances glucose uptake and suppresses oxygen consumption.

(A) Glucose uptake and lactate secretion measured by YSI in *Tsc2*$^{-/-}$ and *Tsc2*$^{+/+}$ MEFs treated with chloroquine (CQ, 5 μM) or control for 24 hours (left panel) or infected with shRNA against

Downloaded from mcr.aacrjournals.org on December 28, 2013. © 2013 American Association for Cancer Research.

Author Manuscript Published OnlineFirst on December 2, 2013; DOI: 10.1158/1541-7786.MCR-13-0258-T
Author manuscripts have been peer reviewed and accepted for publication but have not yet been edited.

the autophagy genes *Atg5* (*Atg5*-1 and *Atg5*-2) or *Beclin1* (right panel). Bars represent average of 4 independent samples ± SD. *p<0.05 **p<0.01

(B) Intact cellular respiration measured using the Seahorse Bioscience XF24 analyzer, under basal conditions or in the presence of FCCP in *Tsc2*$^{-/-}$ MEFs treated with chloroquine (CQ, 5 μM) for 24 hr. Levels of oxygen consumption were normalized to cell number. Bars represent average of 3 independent experiments ± SD. *p<0.05

Figure 3. Autophagy inhibition enhances glucose oxidative metabolism in mTORC1-dependent manner.

(A) Glucose oxidation measured by ^{14}C-CO_2 production in *Tsc2*$^{-/-}$ MEFs following 24-hour treatment with chloroquine (CQ, 5 μM) and 3-hour labeling with D[U-14C]glucose (left panel). Bars represent average of 5 independent experiments ± SD. **p<0.01

(B) Fatty acid oxidation measured by ^{14}C-CO_2 production in *Tsc2*$^{-/-}$ MEFs following 24-hour treatment with chloroquine (CQ, 5 μM) and 3-hour labeling with [U-14C]palmitate (right panel). Bars represent average of 4 independent experiments ± SD. *p<0.05

(C) Glucose oxidation measured by ^{14}C-CO_2 production in *Tsc2*$^{-/-}$ MEFs following 24-hour treatment with chloroquine (CQ, 5 μM), rapamycin (20 nM), or both and 3-hour labeling with D[U-14C]glucose. Bars represent average of 3 independent experiments ± SD. *p<0.05, **p<0.01

(D) Glucose and fatty acid oxidation measured by ^{14}C-CO_2 production in *Tsc2*$^{+/+}$ MEFs following 24-hour treatment with chloroquine (CQ, 5 μM) and 3-hour labeling with D[U-14C]glucose (left panel) or [U-14C]palmitate (right panel). Bars represent average of 3 independent experiments ± SD.

Downloaded from mcr.aacrjournals.org on December 28, 2013. © 2013 American Association for Cancer Research.

Author Manuscript Published OnlineFirst on December 2, 2013; DOI: 10.1158/1541-7786.MCR-13-0258-T
Author manuscripts have been peer reviewed and accepted for publication but have not yet been edited.

Figure 4. Autophagy inhibition and 6-aminonicotinamide act synergistically to suppress the growth of *Tsc2*-null cells.

(A, B) Proliferation of *Tsc2*$^{-/-}$ and *Tsc2*$^{+/+}$ MEFs treated with chloroquine (CQ, 5 μM), 6-aminonicotinamide (6-AN, 10 μM) or both for 4 days, measured by crystal violet staining. Right panel: crystal violet staining. **p<0.01

(C) Proliferation of *Tsc2*$^{-/-}$ and *Tsc2*$^{+/+}$ MEFs treated with the autophagy inhibitor spautin-1 (5 μM), 6-AN (10 μM) or both for 4 days (crystal violet staining). **p<0.01

(D) Proliferation of *Tsc2*$^{-/-}$ MEFs treated with chloroquine (CQ, 5 μM) plus 6-aminonicotinamide (6-AN, 10 μM), NADPH (0.1 mM) alone, or all three for 4 days (crystal violet staining).

Figure 5. Genetic inhibition of macro- or chaperone mediated- autophagy sensitize *Tsc2*-null cells to 6-aminonicotinamide..

(A) Proliferation of *Tsc2*$^{-/-}$ MEFs infected with control shRNA or shRNA against *Atg5* (*Atg5*-1 and *Atg5*-2) or *Lamp2A* and treated with 6-aminonicotinamide (6-AN, 10 μM) for 4 days (crystal violet staining). Time points represent average of 3 independent experiments ± SD. *p<0.05, **p<0.01 (B) Immunoblot analysis of Atg5 (left panel) and Lamp2A (right panel) in shRNA-infected *Tsc2*$^{-/-}$ MEFs.

(C) Autophagy flux analysis in in *Tsc2*$^{-/-}$ MEFs infected with control shRNA or shRNA against *Atg5* (*Atg5*-1 and *Atg5*-2) or *Lamp2A*. Immunoblot analysis of LC3 following 6 hr- treatment with BafilomycinA 20 nM.

Downloaded from mcr.aacrjournals.org on December 28, 2013. © 2013 American Association for Cancer Research.

Author Manuscript Published OnlineFirst on December 2, 2013; DOI: 10.1158/1541-7786.MCR-13-0258-T
Author manuscripts have been peer reviewed and accepted for publication but have not yet been edited.

Figure 6. Combined autophagy and pentose phosphate pathway inhibition lead to activation of NF-kB and the inflammasome.

(A) Immunoblot analysis of phospho-p65 (RelA, ser 536), total RelA, phospho-S6 (ser 235/236) and total S6 in *Tsc2*$^{-/-}$and *Tsc2*$^{+/+}$ MEFs treated with chloroquine (CQ, 5 μM), 6-AN (10 μM) or both for 4 days.

(B) Immunoblot analysis of caspase-1 (pro- and cleaved-form) in *Tsc2*$^{-/-}$ and *Tsc2*$^{+/+}$ MEFs treated with chloroquine (CQ, 5 μM) and 6-AN (10 μM) for 4 days.

(C) Immunoblot analysis of caspase-1 (pro- and cleaved-form) in *Tsc2*$^{-/-}$ MEFs treated with chloroquine (CQ, 5 μM) and 6-AN (10 μM), NADPH (0.1 mM) alone, or all three for 4 days.

(D) Working model: autophagy inhibition enhances ROS production, leading to PPP dependency and inflammasome activation. G6P (glucose-6-phosphate); G6PD (glucose-6-phosphate dehydrogenase); 6P-G (6-phosphogluconate); 6PGD (6-phosphogluconate dehydrogenase); R-5P (ribose-5-phosphate); ROS (reactive oxygen species); CQ (chloroquine); 6-AN (6-aminonicotinamide).

Downloaded from mcr.aacrjournals.org on December 28, 2013. © 2013 American Association for Cancer Research.

Figure 1

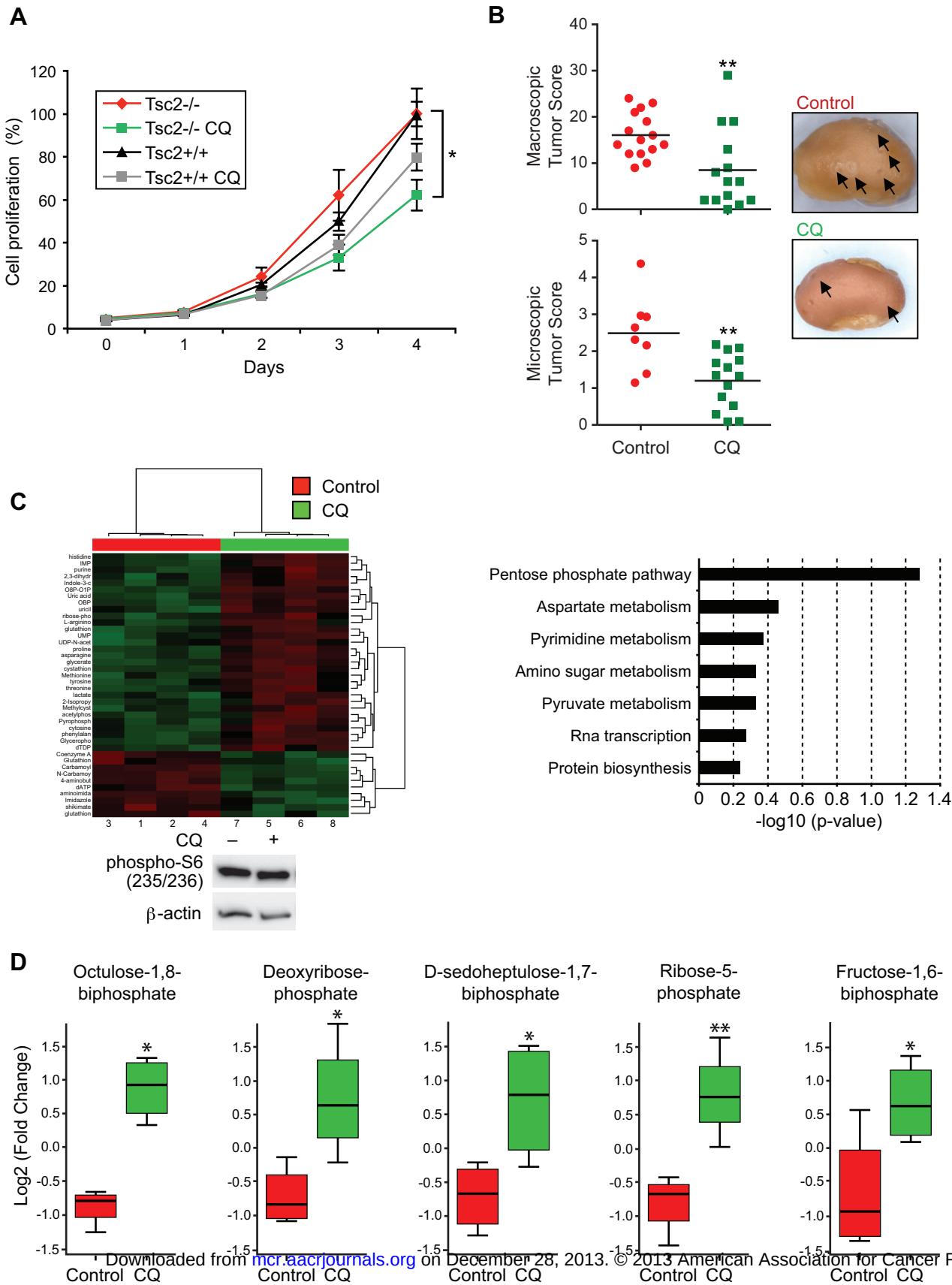

Downloaded from mcr.aacrjournals.org on December 28, 2013. © 2013 American Association for Cancer R

Figure 2

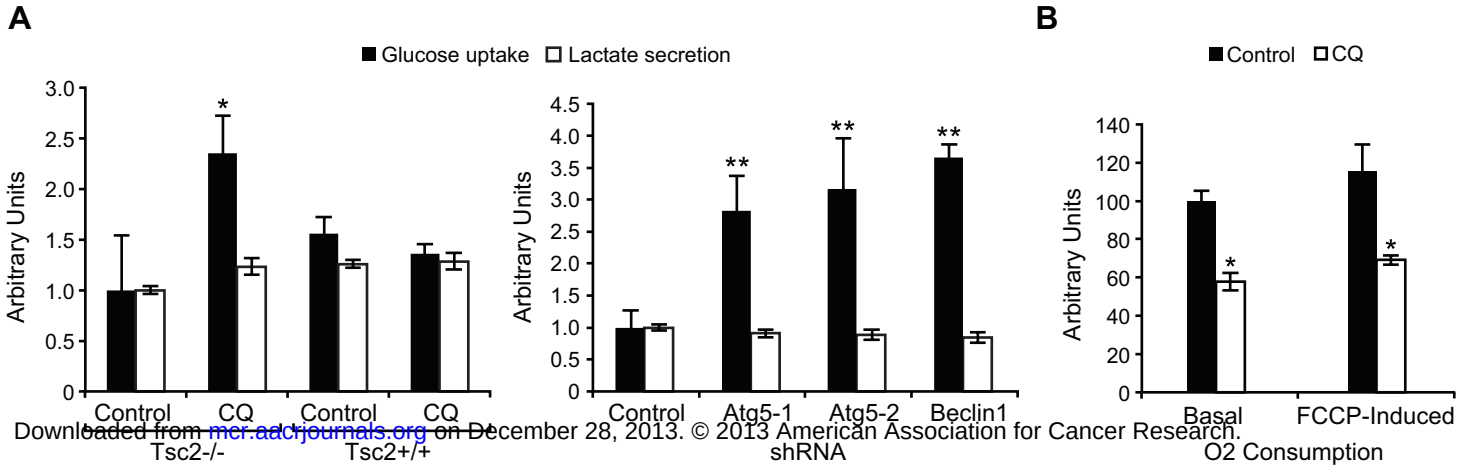

Downloaded from mcr.aacrjournals.org on December 28, 2013. © 2013 American Association for Cancer Research.

Figure 3

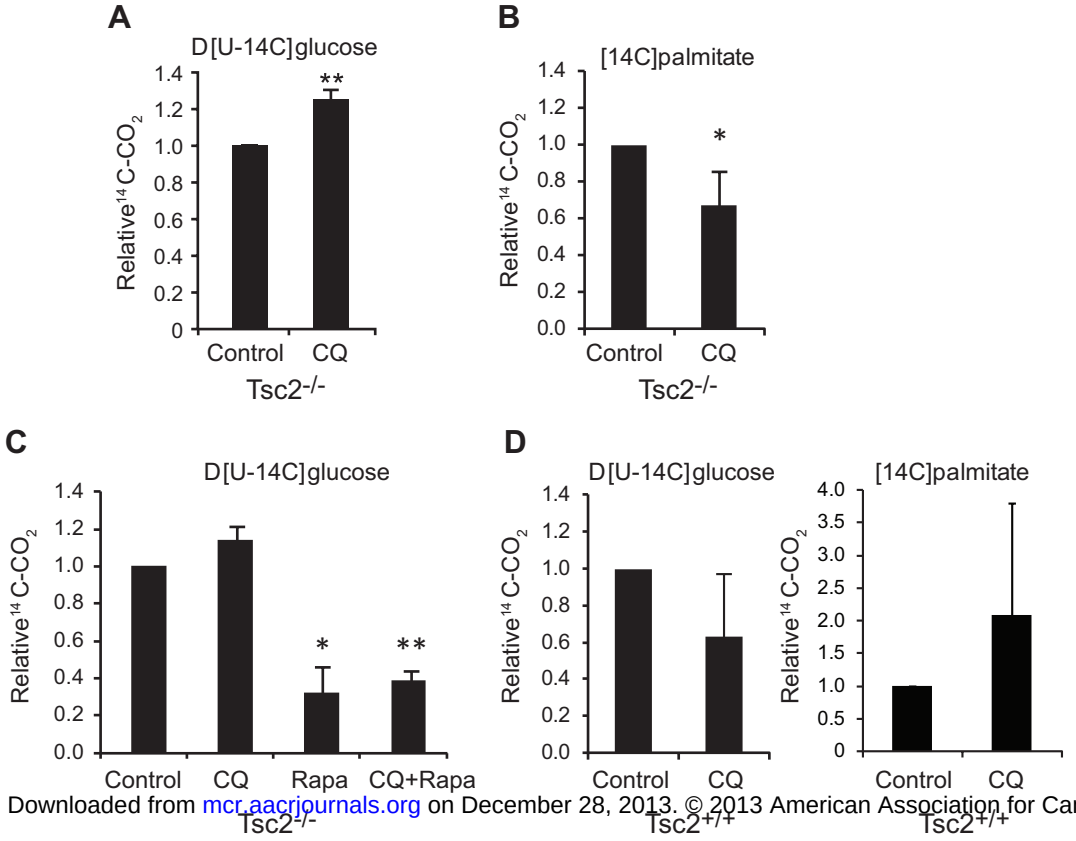

Downloaded from mcr.aacrjournals.org on December 28, 2013. © 2013 American Association for Can

Figure 4

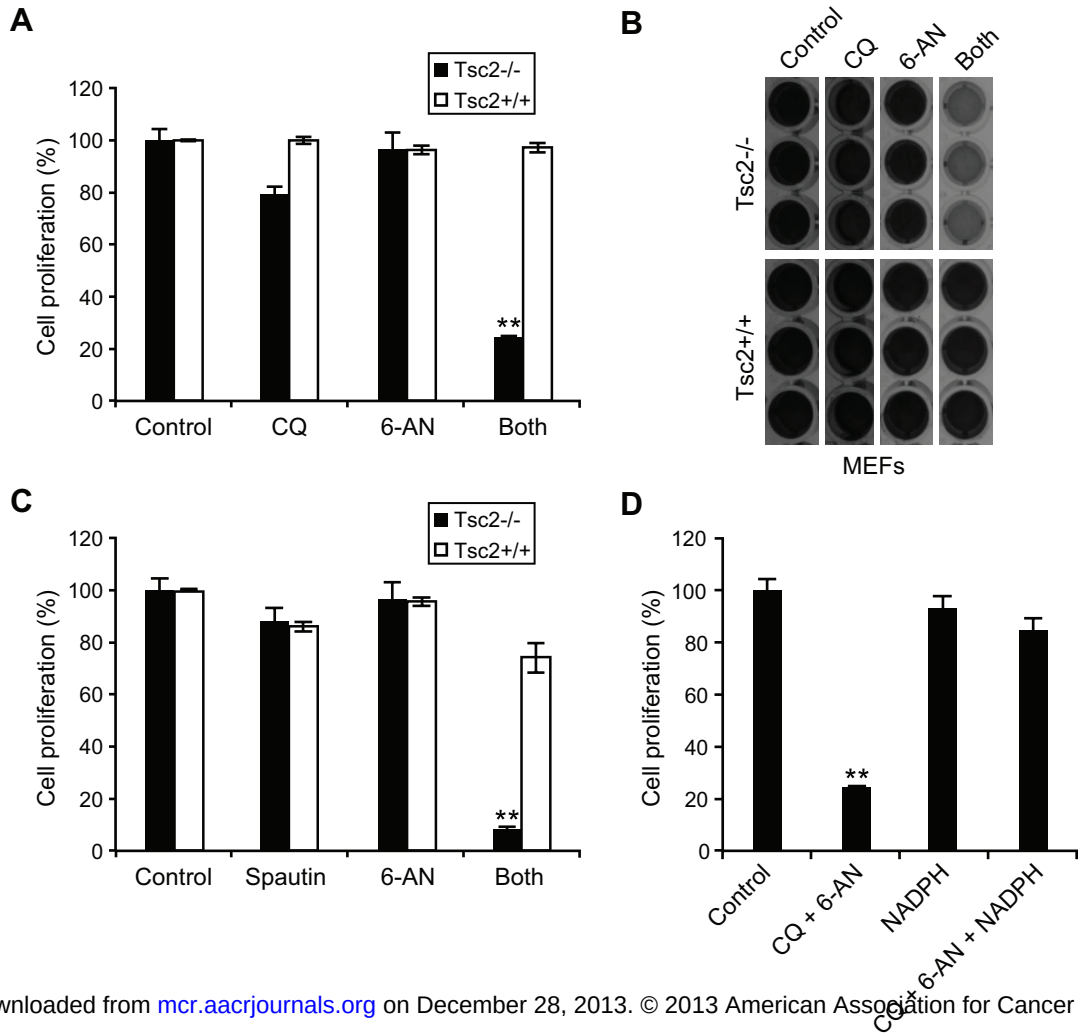

Downloaded from mcr.aacrjournals.org on December 28, 2013. © 2013 American Association for Cancer

Figure 5

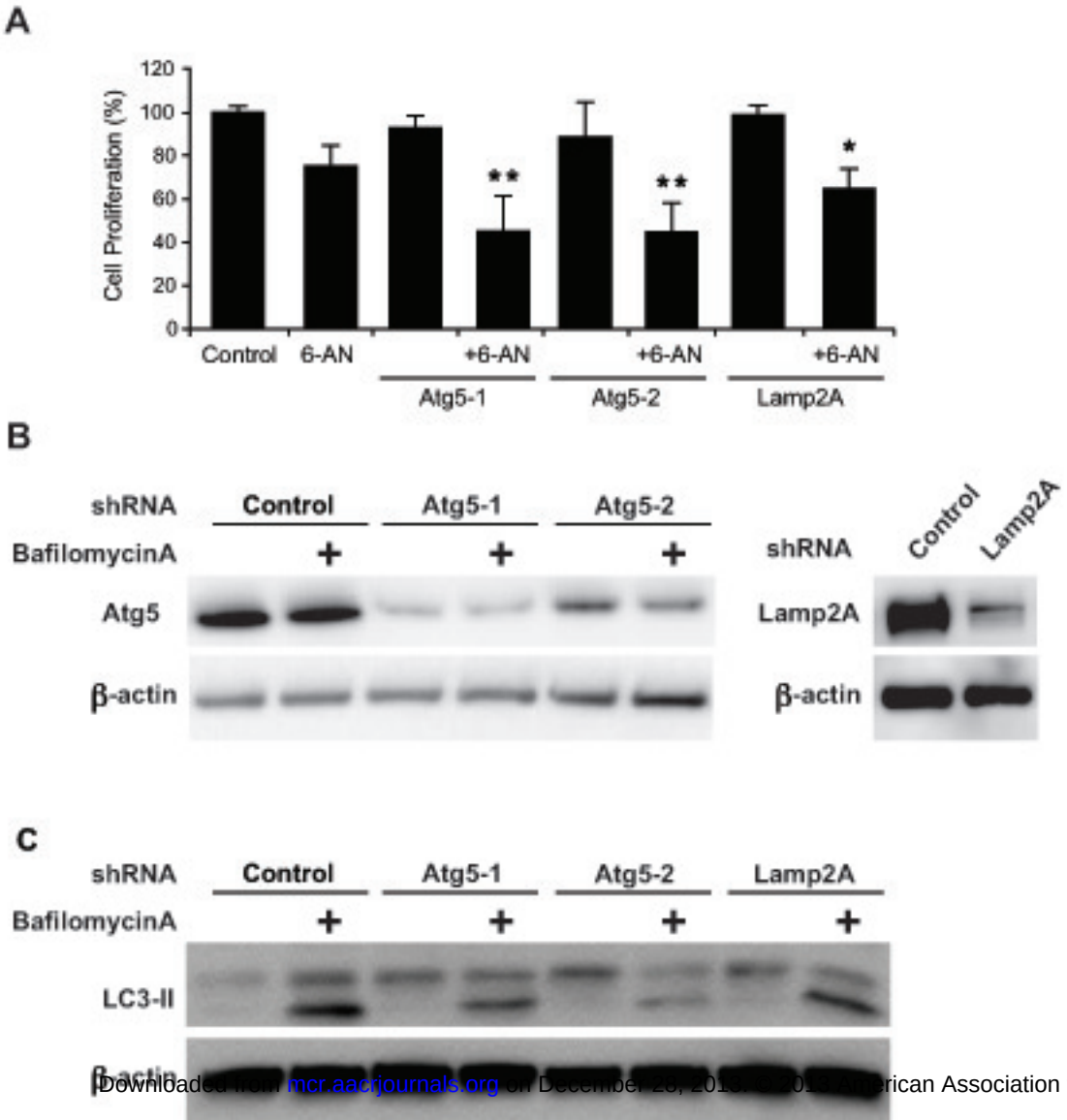

Downloaded from mcr.aacrjournals.org on December 28, 2015. © 2015 American Association

Figure 6

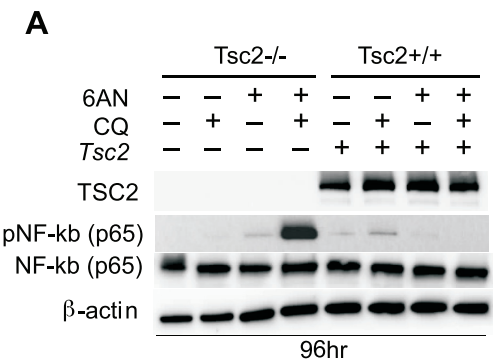

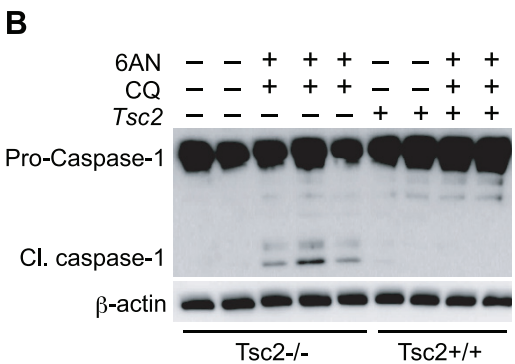

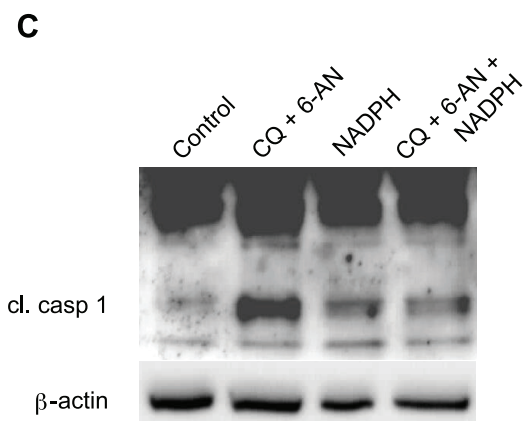

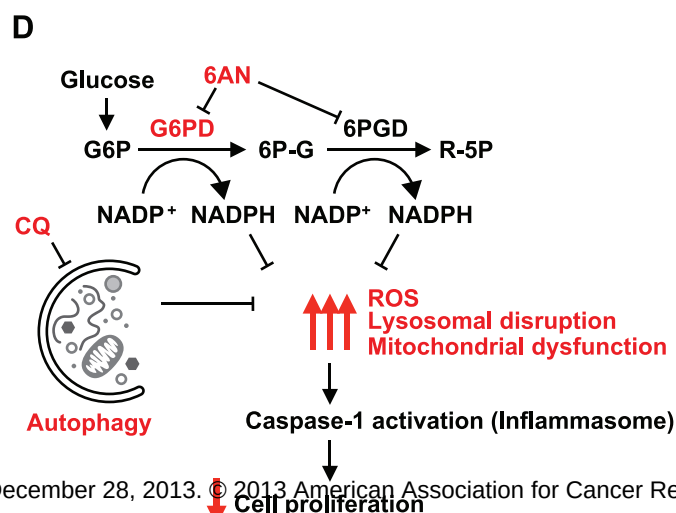

Downloaded from mcr.aacrjournals.org on December 28, 2013. © 2013 American Association for Cancer Re